Cell Insight 5 (2026) 100324

Contents lists available at ScienceDirect

Cell Insight

journal homepage: www.journals.elsevier.com/cell-insight

Research Article

FINE-EM-seq: a rapid isothermal amplification method enabling comprehensive methylome profiling of zebrafish early embryos

Chenyang Ding[a,b,1], Qifeng Zhang[a,1], Jing Wang[a], Yanbo Xu[a], Tiantian Huang[b], Yanfang Du[b], Junjie Zhang[c], Xiang Zhou[b,*], Yibin Liu[b,**], Zhiyuan Hu[a,d,e,f,***]

[a] Reproductive Medicine Center, Medical Research Institute, Frontier Science Center for Immunology and Metabolism, Zhongnan Hospital, Wuhan University, Wuhan, 430072, Hubei, China
[b] State Key Laboratory of Metabolism and Regulation in Complex Organisms, College of Chemistry and Molecular Sciences, Taikang Center for Life and Medical Sciences, Wuhan University, Wuhan, 430072, Hubei, China
[c] State Key Laboratory of Virology and Biosafety, Frontier Science Center for Immunology and Metabolism, Medical Research Institute, Wuhan University, Wuhan, 430071, Hubei, China
[d] Department of Obstetrics, Zhongnan Hospital of Wuhan University, Wuhan, 430071, Hubei, China
[e] Hubei Clinical Research Center for Prenatal Diagnosis and Birth Health, Wuhan, 430071, Hubei, China
[f] Wuhan Clinical Research Center for Reproductive Science and Birth Health, Wuhan, 430071, Hubei, China

HIGHLIGHTS

- FINE enables 20-min isothermal amplification of methylation libraries.
- FINE improves coverage uniformity and methylation accuracy for EM-seq.
- High-coverage profiling reveals methylome dynamics in early development.

GRAPHICAL ABSTRACT

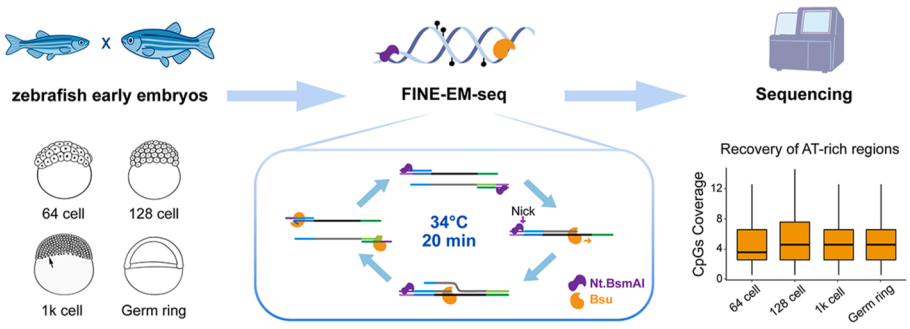

ARTICLE INFO

Keywords:
Isothermal amplification
DNA methylation sequencing
EM-seq
Zebrafish development
AT-rich regions

ABSTRACT

DNA methylation plays a crucial role in development and disease. Bisulfite-free methods such as enzymatic methyl sequencing (EM-seq) offer gentle approaches for whole-genome analysis, but they typically depend on PCR-based library amplification, which distorts coverage and methylation quantification. Here, we introduce FINE (Fast Isothermal amplification via Nicking Enzyme), a robust isothermal amplification strategy that leverages a nicking enzyme-assisted strand displacement reaction and can amplify methylation libraries from sub-nanogram inputs in 20 min. FINE-EM-seq increases library efficiency and coverage uniformity compared to PCR-

* Corresponding author.
** Corresponding author.
*** Corresponding author. Reproductive Medicine Center, Medical Research Institute, Frontier Science Center for Immunology and Metabolism, Zhongnan Hospital, Wuhan University, Wuhan, 430072, Hubei, China.
E-mail addresses: xzhou@whu.edu.cn (X. Zhou), liuyibin@whu.edu.cn (Y. Liu), zhiyuan.hu@whu.edu.cn (Z. Hu).
[1] These two authors contributed equally to this work.

https://doi.org/10.1016/j.cellin.2026.100324
Received 30 December 2025; Received in revised form 12 March 2026; Accepted 2 April 2026
Available online 2 April 2026

based approaches, minimizing amplification bias and improving methylation calling accuracy. Applied to zebrafish embryos at four early developmental stages, FINE-EM-seq characterized stage-associated methylation dynamics through blastulation and early gastrulation. Furthermore, our analysis revealed blastulation-associated differentially methylated regions (DMRs) overlapping with AT-rich regions that were previously under-covered. These results illustrate that FINE-EM-seq is a rapid, robust solution for low-input whole-genome methylation sequencing with broad utility in developmental biology and clinical epigenomics.

1. Introduction

DNA methylation is a key epigenetic modification that regulates gene expression, influences developmental processes, and contributes to disease (Mattei et al., 2022). While bisulfite sequencing (BS-seq) has been the gold standard for base-resolution methylation profiling (Chapin et al., 2022; Lister et al., 2009), its reliance on harsh bisulfite treatment causes significant DNA degradation, material loss, and sequence bias (Du et al., 2023). To mitigate these issues, several gentler methods have been developed, including TET-assisted pyridine borane sequencing (TAPS) (Liu et al., 2019), enzymatic methyl sequencing (EM-seq) (Vaisvila et al., 2021), and ultrafast bisulfite sequencing (UBS-seq) (Dai et al., 2024). However, despite improving the initial DNA conversion step, these methods rely on PCR for library amplification. This step is a major source of bias that distorts methylation profiles and creates uneven genome representation. Specifically, PCR tends to amplify unconverted fragments, leading to inaccurate methylation calling (Kong et al., 2023). In addition, PCR can introduce GC-content-dependent coverage bias (Aird et al., 2011) and suffer from stochastic sampling noise (Kebschull & Zador, 2015) and heat-induced DNA damage due to thermal cycling (Potapov & Ong, 2017).

Through bypassing thermal cycling, isothermal amplification has emerged as a promising alternative to PCR (Asadi & Mollasalehi, 2021; Glökler et al., 2021). While popular diagnostic tools like loop-mediated isothermal amplification (LAMP) and recombinase polymerase amplification (RPA) provide rapid results in resource-limited settings (Daher et al., 2016; Notomi et al., 2015; Srivastava & Prasad, 2023; Tan et al., 2022), they cannot be used for next-generation sequencing due to unspecific amplification products and limited fragment lengths. Two recently developed T7 RNA polymerase-based strategies, namely linear amplification-based bisulfite sequencing (LABS) (Cui et al., 2024) and T7-assisted enzymatic methyl-sequencing (TEAM-seq) (Wang et al., 2022), use *in vitro* transcription (IVT) for template amplification and outperform PCR in fidelity and coverage uniformity, empowering low-input methylome profiling. However, this performance comes at the cost of speed and simplicity. Their multi-step workflows, requiring reverse transcription and second-strand synthesis, are time-consuming and labor-intensive, often involving overnight incubations that limit their use in time-sensitive or high-throughput settings. Other strategies like multiple displacement amplification (MDA), although effective for single-cell applications (Dean et al., 2002), are incompatible with converted DNA used in methylation analysis (Wang et al., 2022). Therefore, there is a critical need for an amplification strategy that reconciles high-fidelity profiling with a streamlined, cost-effective workflow compatible with converted DNA.

To address these limitations, we developed Fast Isothermal amplification via Nicking Enzyme (FINE), a rapid and low-bias strategy for methylome library amplification. FINE combines a strand-displacing DNA polymerase with a site-specific nicking enzyme to achieve exponential amplification in just 20 min under isothermal conditions. The overall FINE-EM-seq workflow, which integrates enzymatic conversion, is streamlined and minimizes amplification bias. In a direct comparison with conventional PCR, FINE-EM-seq achieved higher mapping efficiency, more uniform GC coverage, and higher methylation calling accuracy.

To demonstrate its utility, we applied FINE-EM-seq to zebrafish embryos across four early developmental stages. Unlike mammals, zebrafish methylomes remain globally stable during early development (Jiang et al., 2013; Potok et al., 2013), but undergo subtle, functionally important changes linked to zygotic genome activation (ZGA) (Schulz & Harrison, 2019; Wu et al., 2021). Previous whole-genome methylation studies provided key insights into early epigenetic reprogramming, revealing the inheritance of paternal methylation patterns and stage-specific regulatory features (Andersen et al., 2012; Jiang et al., 2013; Potok et al., 2013). However, they relied on PCR-amplified whole-genome bisulfite-sequencing (WGBS) methods such as MethylC-seq (Urich et al., 2015), which are known to underrepresent AT-rich and other challenging genomic regions, potentially obscuring key regulatory events (Du et al., 2023; Olova et al., 2018; Oyola et al., 2012). By overcoming these limitations, FINE-EM-seq efficiently recovered low-GC regions with high accuracy, enabling a more complete and more balanced view of the methylation dynamics underlying blastulation and early gastrulation. It also revealed stage-associated regulatory changes, including DMRs overlapping with AT-rich regions that were under-covered in previous studies.

2. Results

2.1. Development of the FINE system

We screened isothermal amplification strategies for methylome library preparation. Common methods, e.g., LAMP, RPA, and strand displacement amplification (SDA), are ill-suited for this purpose (Srivastava & Prasad, 2023). They frequently yield non-specific products and fail to produce long DNA fragments required for sequencing (Song et al., 2023; Zyrina & Antipova, 2021). In contrast, nicking-enzyme-assisted amplification (NEAA) (Qian et al., 2019), exemplified by palindrome-nicking-dependent amplification (PaNDA) (Wang et al., 2024), uses a site-specific nick to create a defined 3′-OH starting point for polymerases, thereby enabling controlled and specific initiation. To implement this principle, we optimized the enzymatic cocktail from two aspects. First, to reduce non-specific synthesis observed with the commonly used Bst DNA polymerase (Zyrina & Antipova, 2021), we selected Bsu DNA polymerase for its higher specificity (Zhang et al., 2024; Zyrina & Antipova, 2021). Second, to suppress background amplification and stabilize the reaction, we incorporated single-stranded DNA-binding protein T4 gp32 (Reid et al., 2018; Zhang & Tanner, 2017; Zyrina et al., 2012) and PEG8000 (Bagnoli et al., 2018; Hu et al., 2020; Sasaki et al., 2006), which together promote accurate primer-template annealing and enhance polymerase processivity.

This optimized system, named Fast Isothermal amplification via Nicking Enzyme (FINE), enables efficient library amplification in a self-sustaining cycle (Fig. 1(A)). This process starts with a standard library of DNA fragments ligated with conventional Y-shaped adapters. The amplification cycle of these DNA fragments is initiated when primers, blocked at their 3′ ends with amine modifications to prevent self-extension, anneal to the adapter regions. Bsu DNA polymerase then fills in the 5′ overhang, creating a double-stranded recognition site for the nicking enzyme Nt.BsmAI. Nt.BsmAI introduces a site-specific nick, generating a fresh 3′-OH terminus (Zhu et al., 2004). From this nick, Bsu DNA polymerase begins strand-displacement extension, creating a new strand while peeling away the existing one. This newly displaced single strand becomes a fresh template for the next round of primer annealing, triggering a continuous, exponential amplification cascade under isothermal conditions.

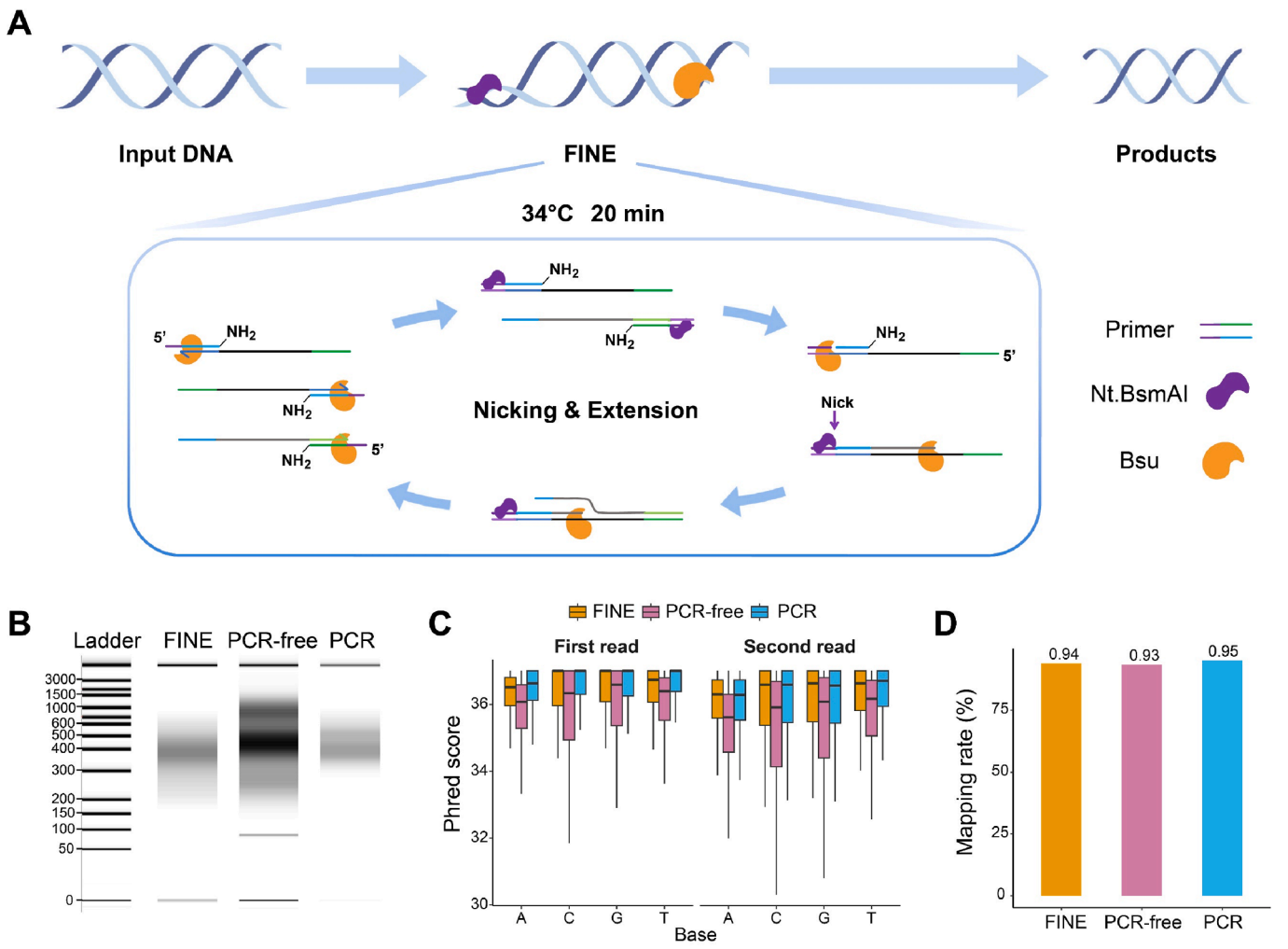

Fig. 1. Overview of Fast Isothermal amplification via Nicking Enzyme (FINE) and its sequencing performance. (A) Schematic of FINE, illustrating primer binding, nicking by Nt.BsmAI, strand extension by Bsu polymerase, and iterative amplification cycles. FINE, PCR-free, and PCR libraries were compared for library quality, including **(B)** library size distribution measured by LabChip GX bioanalyzer, **(C)** base quality scores across four nucleotides, where the horizontal line within each box denotes the median, box edges correspond to the 25th and 75th percentiles, and whiskers extend to 1.5 × the interquartile range (IQR), and **(D)** mapping rates to the reference genome.

As a proof-of-concept experiment, we used FINE to amplify standard genomic libraries and benchmarked its performance. We prepared sequencing libraries from 1 ng of sheared HeLa genomic DNA, which was then amplified with either FINE or conventional PCR. A PCR-free library prepared from a high-input (200 ng) sample served as a reference control. Key quality metrics were comparable across all methods (Table S1). The FINE-amplified libraries displayed a fragment size distribution similar to the PCR and PCR-free methods (Fig. 1(B)), exhibited excellent base-quality scores (Fig. 1(C)), and achieved nearly identical mapping rates (Fig. 1(D)). The PCR-free library exhibited modestly lower base quality scores compared to the FINE and PCR-amplified libraries (Fig. 1(C)), most likely attributable to residual adapter dimers and short ligation products, which were detectable by capillary electrophoresis during library quality control (Fig. 1(B)). Although double-sided bead cleanup was performed following adapter ligation, such short species are more likely to persist in a PCR-free workflow because of the absence of post-amplification enrichment or a secondary size selection step.

While a local reduction in read depth was observed specifically around endogenous GTCTC motifs, the recognition sites of Nt.BsmAI, in unconverted WGS libraries (Fig. S1A), no such signature was observed around GTTTT, the theoretical product expected after C-to-T conversion of GTCTC (Fig. S1B). These results indicate that the motif-associated depletion effect arises from intact Nt.BsmAI recognition sites present in native genomic DNA. Consequently, FINE is not ideally suited for standard WGS applications, which require unbiased representation of unconverted genomes. In contrast, for conversion-based methylation sequencing, C-to-T conversion removes most susceptible GTCTC motifs, thereby largely bypassing this sequence-dependent coverage bias.

2.2. *FINE outperforms PCR in EM-seq library amplification*

To benchmark FINE against PCR for EM-seq library amplification, we used converted HeLa genomic DNA across three input levels: 1 ng, 100 pg, and 10 pg. For FINE, two independent library preparations followed by independent isothermal amplifications were performed at each input level to assess reproducibility. While the number of PCR cycles required optimization for each input level (16, 20, or 23 cycles, respectively), the FINE reactions were performed under a single, universal condition (20 min at 34 °C), highlighting the simplicity and input-independent robustness of FINE (Fig. 2(A); Fig. S2).

In terms of sequencing data quality, FINE performed well relative to PCR. At 1 ng input, performance was broadly comparable with a slight advantage for FINE, and differences became more apparent at lower inputs (Table S2). FINE yielded robust mapping efficiency of around 80% across all input levels, whereas the mapping efficiency of PCR

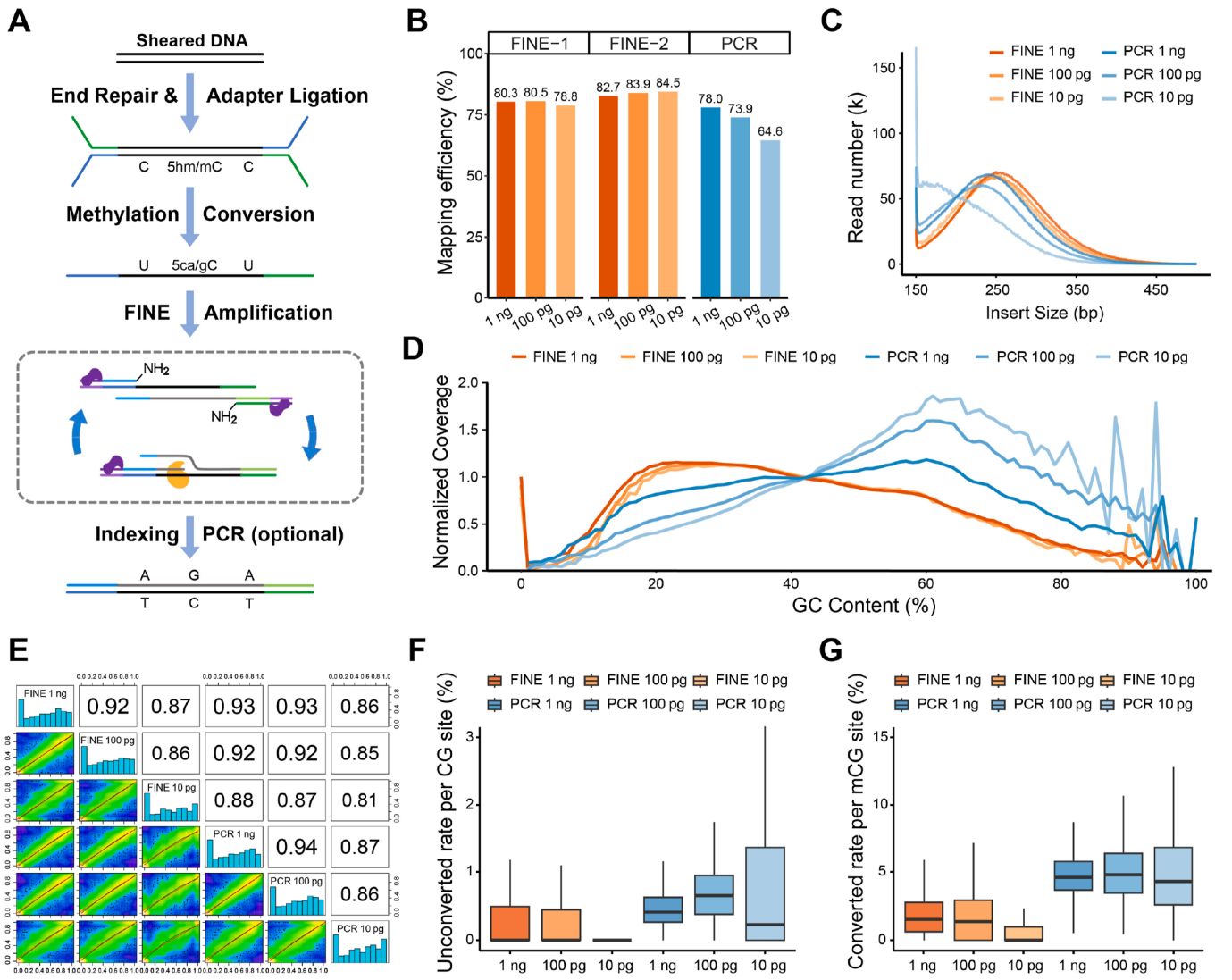

Fig. 2. Benchmarking library quality between PCR and FINE-EM-seq across DNA input levels. (A) Schematic of FINE-EM-seq. **(B)** Mapping efficiency (% of aligned reads by Bismark). **(C)** Insert size distribution. **(D)** Normalized genome coverage across GC-content bins, where coverage in each bin was normalized to its genomic representation. **(E)** Pairwise Pearson correlation coefficients of CpG methylation levels (coverage ≥ 3) between two methods. Site-specific methylation detection error rates were evaluated using two spike-in controls, including **(F)** unconverted rates of unmethylated CpG sites and **(G)** falsely converted rates of methylated CpG sites.

libraries declined as input decreased (Fig. 2(B)). Insert-size distributions were stable for FINE but shifted towards shorter fragments for PCR at low input (Fig. 2(C)). Similarly, at 1 ng input, the GC-coverage profiles of FINE and PCR were broadly comparable. FINE retained relatively better coverage in low-GC regions and showed more consistent profiles across inputs, whereas PCR profiles varied with input, consistent with GC-dependent effects of thermal cycling (Aird et al., 2011; Feng et al., 2020; Oyola et al., 2012) (Fig. 2(D)). Moreover, genome coverage breadth (≥ 1 ×) was modestly higher for FINE than for PCR across inputs (Fig. S3; Table S2). As the input amount decreased, both methods showed a gradual reduction in genome coverage breadth, reflecting the constraints of limited starting material (Kebschull & Zador, 2015) rather than the amplification chemistry.

We then quantified methylation levels across the genome and spike-in sequences. Between PCR and FINE, the genome-wide per-CpG methylation levels were highly correlated (r = 0.81-0.94), demonstrating overall consistency between the two amplification methods (Fig. 2(E)). Moreover, independent FINE-EM-seq replicates showed high concordance of genome-wide CpG methylation levels, with Pearson correlation coefficients of 0.91 at 1 ng, 0.90 at 100 pg, and 0.83 at 10 pg, supporting reproducible methylation profiling across the tested input range, including ultra-low-input samples (Fig. S4). To assess methylation profiling accuracy, an unmethylated spike-in was used to estimate the unconverted rate of unmethylated cytosines (false-positive rate), and a CpG methylated spike-in was used to estimate the converted rate of methylated CpGs (false-negative rate). FINE libraries showed lower error rates than PCR libraries across input levels (Fig. 2(F) and (G)). We reasoned that these higher false positive and false negative error rates of PCR were caused by the preferential amplification of unconverted cytosines (Feng et al., 2020; Ji et al., 2014) and heat-induced deamination of modified cytosines during thermal cycling (Lewis et al., 2016; Potapov & Ong, 2017), respectively. Comparisons with PCR-based EM-seq libraries generated with 2 × Syn (2 × Synthesis Mix), KAPA U (KAPA HiFi HotStart Uracil + ReadyMix), and HiFi V3 polymerases showed that KAPA U yielded mapping efficiency similar to FINE-EM-seq and higher than 2 × Syn and HiFi V3 (Fig. S5A). However, duplication rates and methylation profiles varied across polymerases and input levels (Fig. S5B–C). In particular, under low-input conditions (100 pg and 10 pg), FINE-EM-seq maintained stable CpG methylation with lower non-CpG background across gene bodies and their ±2 kb flanking

regions (Fig. S5C). Together, these observations support that the improved performance of FINE-EM-seq at low inputs is not attributed solely to the selection of amplification polymerase.

2.3. FINE-EM-seq enables high-fidelity methylome profiling of early zebrafish development

To assess the performance of FINE-EM-seq for methylome profiling in biological samples, we analyzed zebrafish early embryos across a developmental window marked by widespread transcriptional activation (Jukam et al., 2017). Through these stages, many loci undergo subtle DNA methylation changes critical for biological processes like ZGA (Jiang et al., 2013; Potok et al., 2013). For example, the *hoxb1a* and *hoxb3a* promoters demethylate from cleavage to gastrulation to gain transcriptional competency (Potok et al., 2013). However, accurate profiling of methylome changes is often confounded by PCR amplification biases (Aird et al., 2011; Kebschull & Zador, 2015; Olova et al., 2018).

We therefore applied FINE-EM-seq to four key developmental stages, including the 64-cell, 128-cell, 1k-cell and Germ-ring stages, using 1 ng of input DNA per sample (Table S3). The global methylation levels profiled by FINE-EM-seq remained stable, with a modest increase across stages (Fig. 3(A)). Despite the low input, FINE-EM-seq libraries achieved high mapping efficiency and broad, uniform CpG coverage. To distinguish biological validation from technical benchmarking, we compared FINE-EM-seq and PCR-EM-seq libraries generated from the same zebrafish embryo DNA under identical enzymatic-conversion conditions and analyzed them at matched sequencing depth (~3 Gb per library). Across all stages, PCR-EM-seq libraries showed consistently higher duplication rates and lower deduplicated genome coverage than FINE-EM-seq (Fig. S6, Table S4), indicating improved library complexity with FINE amplification under otherwise identical EM-seq conditions. Published zebrafish WGBS datasets were considered separately as biological reference methylomes for early embryonic development (Jiang et al., 2013) (Fig. 3(B) and (C); Fig. S7). Across the four developmental stages, FINE-EM-seq libraries generally covered more CpG sites than the published WGBS reference datasets, except at the 1k-cell stage where coverage was comparable. At the same time, the stage-specific methylation patterns observed by FINE-EM-seq were consistent with previously described developmental methylation dynamics. In an 80-kb region spanning the *hoxb* cluster, FINE-EM-seq also showed uniform coverage across replicates (Fig. 3(C)). Furthermore, biological replicates were highly consistent for FINE-EM-seq with the Pearson correlation coefficients between 0.86 and 0.92 (Fig. S8). Together, these results demonstrate the robustness of FINE-EM-seq in a matched technical comparison with PCR-EM-seq and support the reliability of the resulting zebrafish methylome datasets for investigating early embryonic development in the context of established reference methylomes.

To identify stage-specific methylation changes related to blastulation and early gastrulation, we performed DMR analysis between 64-cell, 128-cell, 1k-cell, and Germ-ring stages. In total, 12 375 to 14 109 stage-specific hypomethylated regions (hypo-DMRs) were identified per comparison using MethylKit (Akalin et al., 2012) ($meth.diff \leq -10$, $q \leq 0.05$). Genomic annotation revealed that approximately one-third of hypo-DMRs overlapped with gene body regions, mostly in intronic (14.3%–15.3%) and promoter (14.4%–16.4%) regions (Fig. 3(D)). In the Germ-ring versus 64-cell comparison, 9 720 of 14 109 hypo-DMRs were positioned at least 10 kb from the nearest gene, with most of them (7 671 of 9 720) located in intergenic regions (Fig. S9).

To explore biological functions of these genomic regions, we annotated DMRs to DMR-associated genes, i.e., genes harboring DMRs in putative promoters and genebody regions, and performed Gene Ontology enrichment analysis. In the Germ-ring versus 64-cell comparison, DMR-associated genes were enriched in biological processes such as GTP metabolic process and calcium-dependent cell-cell adhesion via plasma membrane cell-adhesion molecules (BH-adjusted $p < 0.05$) (Fig. 3(E)). These enrichments were consistent with the increased metabolic activity (Stackley et al., 2011) and cadherin-mediated adhesion driving cell rearrangements during epiboly and gastrulation (Bruce & Heisenberg, 2020; Kane et al., 2005; Shimizu et al., 2005). Neurogenesis-related processes were also enriched, suggesting the epigenetic changes preceding the onset of neurodevelopmental programs during gastrulation (Schmidt et al., 2013). At the locus level, we detected hypo-DMRs (Germ ring vs 64-cell) near *dync1li1*, orthologous to human *DYNC1LI1*, which encodes a component of the cytoplasmic dynein motor complex (Tan et al., 2011) involved in microtubule-based transport (Reck-Peterson et al., 2018) (Fig. 3(F)). We also observed stage-specific methylation changes near *sox19a*, a SoxB1 transcription factor expressed during blastula and gastrula stages, aligning with its role in ZGA (Lee et al., 2013) and neural induction (Okuda et al., 2006) (Fig. 3(F)). Finally, several members of the Hox clusters, canonical regulators of anterior-posterior patterning in vertebrates (Yamada et al., 2021), exhibited stage-associated methylation changes, in line with their known regulatory roles in early embryogenesis (Potok et al., 2013) (Fig. S10).

2.4. Uniform coverage by FINE-EM-seq improves detection of DMRs in AT-rich regions

Having established improved library complexity relative to matched PCR-EM-seq (Fig. S6), we next asked whether this improved coverage uniformity expanded biological readout in genomic regions that were underrepresented in previously available zebrafish reference methylomes.

In zebrafish, AT-rich regions (GC content < 25%) account for more than 10% of the whole genome when scanned using 100-bp bins (Fig. S11). However, such low-GC regions were underrepresented in the previously published zebrafish WGBS reference datasets (Jiang et al., 2013) (Fig. 4(A)). By contrast, FINE-EM-seq provided more uniform coverage across GC content, improving representation of AT-rich regions and thereby expanding access to developmentally relevant loci in these genomic contexts (Fig. 4(A)). We observed differences in GC-bias profiles between HeLa and zebrafish datasets (Figs. 2(D) and 4(A)). As the GC-bias profiles are normalized coverage across GC-content bins, not as absolute measures of amplification efficiency (Benjamini & Speed, 2012), the differences reflected not only library chemistry but also the GC-window distribution and sequence composition of the corresponding reference genomes, rather than the species-specific shift in the intrinsic behavior of FINE-EM-seq. In pairwise stage comparisons, 34.0%–35.6% (mean 34.6%) of identified hypo-DMRs contained at least one AT-rich 100-bp bin with ≥ 1 CpG site (4.4k–4.8k per differential analysis), indicating that AT-rich regions are important for DMR detection (Fig. 4(B)). At base-resolution, 36 775 CpG sites within hypo-DMRs overlapped AT-rich regions. For these CpG sites, the per-site coverage in FINE-EM-seq samples (3.74–4.69 ×) was markedly higher than the WGBS datasets (0.21–3.40 ×) (Fig. 4(C)).

An example was at the promoter of *acvr1l* (*alk8*), a BMP type-I receptor essential for dorsoventral patterning in zebrafish (Bauer et al., 2001; Mintzer et al., 2001). A hypo-DMR (Germ ring vs 64 cell) at this promoter overlapped with an AT-rich region, which harboured a CpG site with changing methylation levels (Fig. 4(D)). Moreover, within this AT-rich region, FINE-EM-seq achieved robust coverage (above 3 ×) at this CpG site, whereas the published WGBS reference data provided more limited coverage. This improved coverage enabled estimation of methylation dynamics at an AT-rich developmental locus that was less accessible in the reference datasets, underscoring the biological value of more uniform methylome profiling in zebrafish early development.

3. Discussion

DNA methylation sequencing from low-input samples has long been constrained by a trade-off between coverage uniformity, data accuracy,

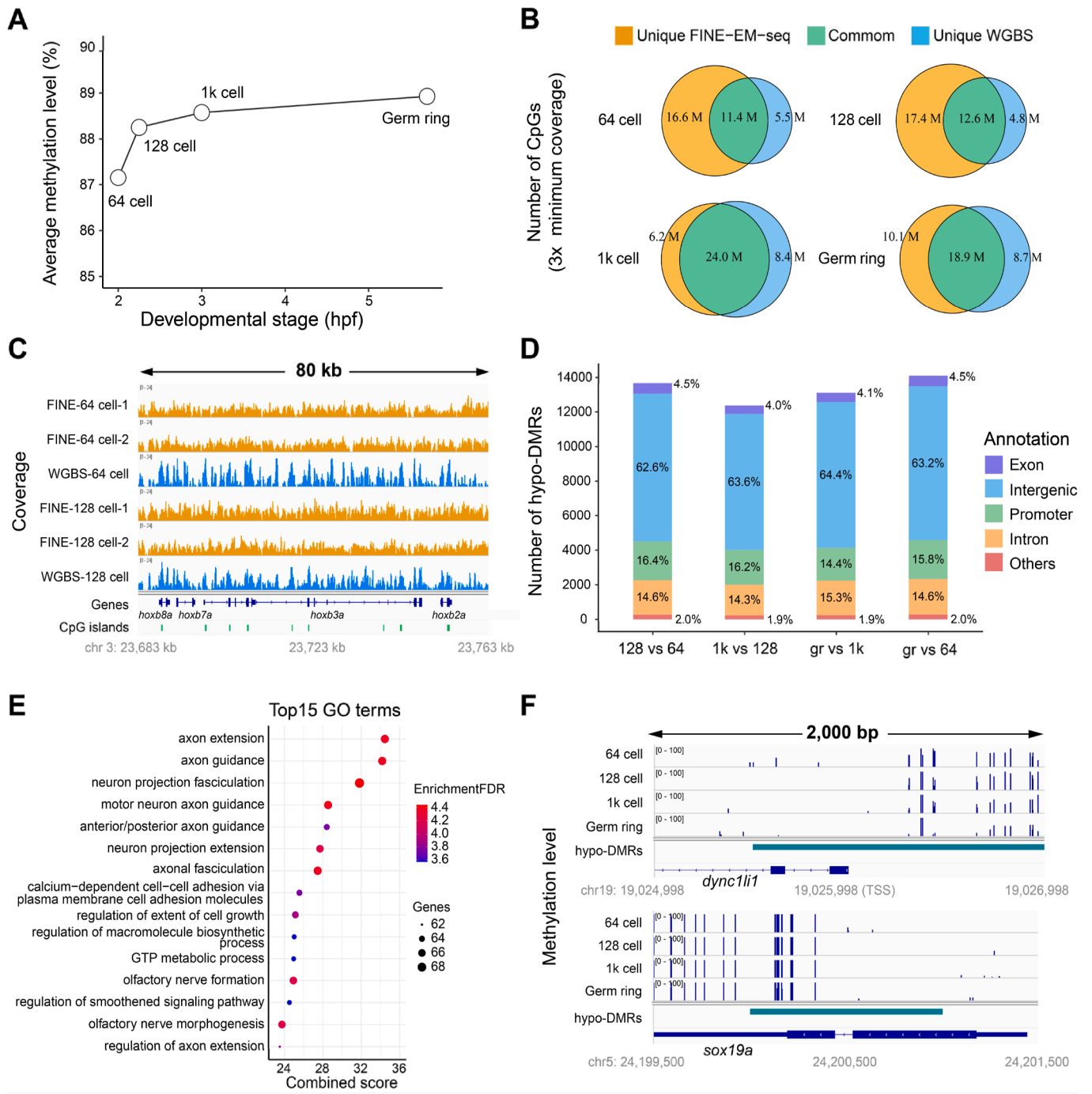

Fig. 3. Methylome profiling of zebrafish embryos using FINE-EM-seq. (A) Global CpG methylation levels across four early developmental stages (64 cell, 128 cell, 1k cell, and Germ ring). Hour post fertilization, hpf. **(B)** Comparison of CpGs covered by at least three reads between FINE-EM-seq and WGBS libraries at each stage, with unique and shared sites represented by Venn diagrams. **(C)** Genome browser view of an 80-kb region encompassing the hoxb cluster, comparing coverage from FINE-EM-seq (orange) and published WGBS data (blue). **(D)** Genomic distribution of hypomethylated regions (hypo-DMRs) identified in differential analyses between stages. Gr, Germ ring. **(E)** Gene Ontology enrichment analysis of DMR-associated genes in the Germ-ring versus 64-cell comparison. **(F)** Two examples of hypo-DMRs (Germ ring vs 64 cell) overlapping the promoter of *dync1li1* and the gene body of *sox19a*, respectively.

and workflow practicality. Here we present FINE, a 20-min isothermal method that generates high-quality methylation libraries from sub-nanogram inputs. By replacing conventional multi-cycle PCR amplification and avoiding complex multi-step enzymatic reactions, FINE streamlines library preparation, reduces amplification bias, and minimizes material loss, all at a low per-sample cost (Table S5).

The superior performance of FINE stems from its unique enzyme-driven, isothermal mechanism. The process relies on the coordinated activity of Bsu DNA polymerase, which is well-suited for AT-rich converted DNA, and the nicking enzyme Nt.BsmAI, which creates specific 3′ initiation sites for continuous, controlled amplification. This design is the foundation for the method's accuracy and uniformity. Unlike PCR, FINE operates at a constant low temperature, thereby avoiding heat-induced DNA damage and reducing cytosine deamination, a major source of artefacts in methylation analysis. Furthermore, the controlled initiation from specific nicks, combined with additives (e.g., T4 gp32) that resolve secondary structures, mitigates the stochastic biases and GC-dependent amplification seen in PCR. Together, these

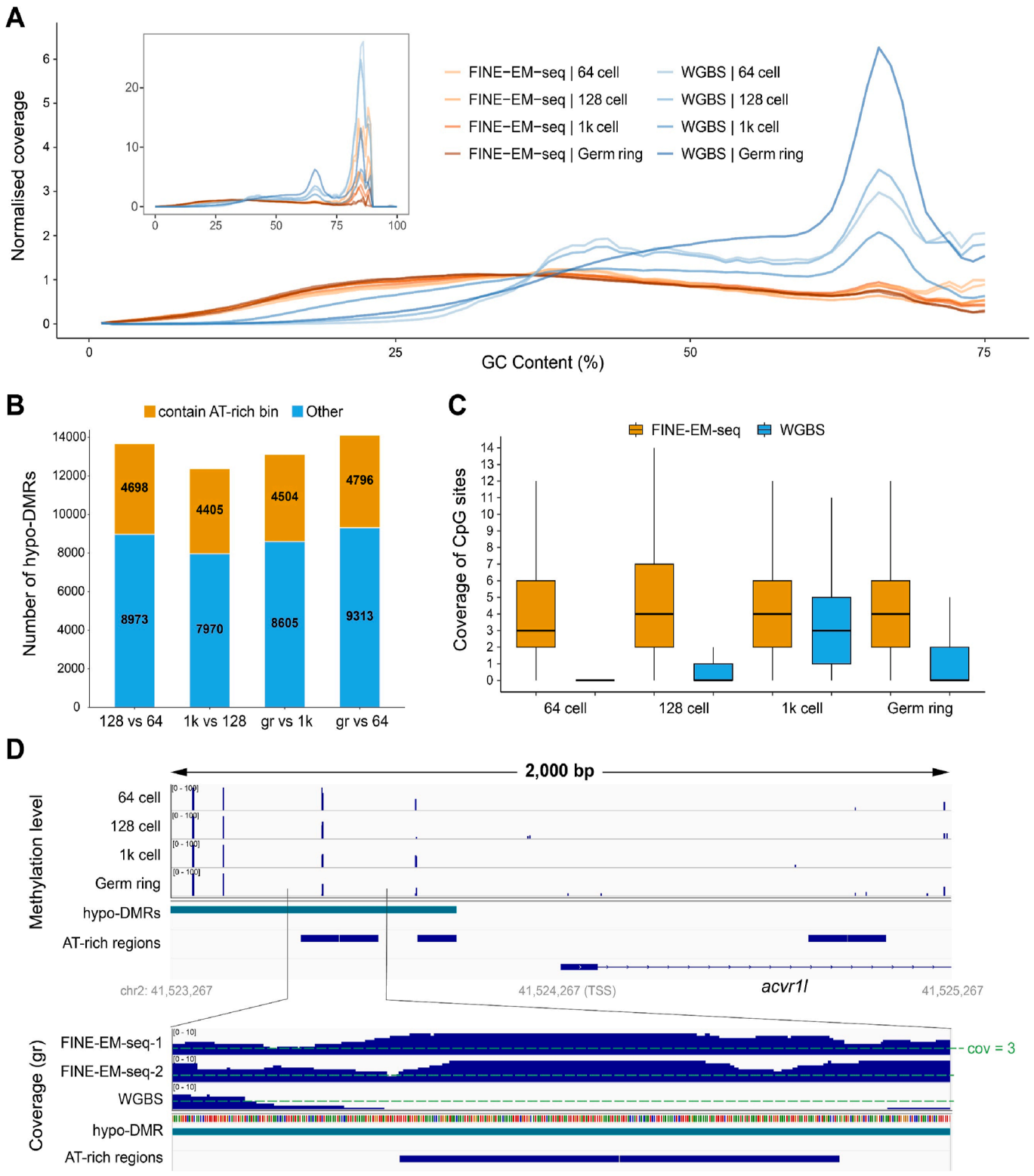

Fig. 4. Uniform coverage across GC content of FINE-EM-seq improves DMR detection. (A) Normalized coverage across genomic regions binned by GC content for FINE-EM-seq and published WGBS libraries at four developmental stages, with coverage in each GC bin normalized to its representation in the reference genome. The main panel shows the 0–75% GC range, while the inset displays the full 0–100% range, including the rare high-GC bins (>75%, ~0.02% of the genome). **(B)** Distribution of hypo-DMRs that contain at least one AT-rich 100-bp bin with ≥ 1 CpG site, compared to those without, in pairwise stage comparisons. **(C)** Per-CpG coverage for sites located in AT-rich regions that intersect with hypo DMRs, compared between FINE-EM-seq and WGBS libraries across four stages. **(D)** Example locus near the *acvr1l* promoter, where an AT-rich region overlaps with a hypo-DMR (Germ ring, gr vs 64 cell). CpG methylation levels (top) and coverage tracks (bottom) are shown; dashed line marks coverage ≥ 3.

features result in better coverage uniformity, which is critical for accurate profiling of challenging genomic regions.

The application of FINE-EM-seq to zebrafish early embryos showcases its power to characterize complex biological processes, such as subtle epigenetic reprogramming in development. Our method not only used fewer embryos and required lower sequencing depth than previous studies, but also yielded datasets with better coverage uniformity across GC content. This success in resolving epigenetic dynamics within previously underrepresented genomic regions validates that FINE-EM-seq preserves authentic biological signals from low-input samples.

Despite its advantages, FINE has several limitations. First, although the short Nt.BsmAI recognition site (GTCTC) is not an issue for methylation libraries where the unmethylated cytosines in these sites are converted, it can cause off-target cleavage for applications such as whole-genome sequencing and TAPS, leading to a local reduction in coverage around GTCTC motifs. Second, as an exponential process, FINE reduces amplification bias but does not fully overcome the limitations associated with picogram-level input (Kebschull & Zador, 2015), leading to a decline in performance, especially at 10 pg input.

Looking ahead, the speed, simplicity, and accuracy of FINE provide exciting opportunities for technical refinement and broader applications. A key frontier is pushing the sensitivity to the true single-cell level, optimizing the library construction strategies (Gansauge et al., 2017; Gansauge & Meyer, 2013) and integrating with microfluidic platforms (Lim et al., 2024). Beyond sensitivity, FINE's gentle, low-temperature chemistry is ideal for challenging sample types like circulating cell-free DNA (cfDNA), FFPE tissues, and ancient DNA, where traditional workflows often fail (Gansauge et al., 2017; Gansauge & Meyer, 2013). Its constant-temperature format also lends itself to automation and point-of-care applications. With continued development, we envision FINE evolving into a versatile platform technology, empowering low-input epigenomics and enabling rapid, cost-effective methylation profiling across a wide range of research and clinical settings.

4. Materials and methods

4.1. Preparation of spike-in controls

Two 2-kb DNA spike-in controls, designated 2kb-2 and 2kb-3, were generated by PCR amplification from the pNIC28-Bsa4 plasmid (Addgene, 26103) as described previously (Liu et al., 2019) (sequences of primers listed in Table S6). To generate a fully CpG-methylated spike-in control, the 2kb-2 amplicon was treated with M.SssI CpG methyltransferase (NEB, M0226), according to a published protocol (Liu et al., 2019), while 2kb-3 remained untreated and was used as the unmethylated control. Both spike-in controls were added at 0.075% of the total DNA input to each library. The spike-in DNAs were fragmented to an average size of ~300 bp using a Covaris M220 Focused-ultrasonicator. The sequences of both spike-in controls are provided in the Supplementary Information.

4.2. Cell culture and genomic DNA isolation

HeLa cells were cultured in a humidified incubator (ESCO Cellmate, CLM-170B-8-NF) at 37 °C with 5% CO_2. The cells were maintained in Dulbecco's Modified Eagle Medium (DMEM; Invitrogen, 11965092) supplemented with 10% fetal bovine serum (FBS; Invitrogen, A5670701) and 1% Penicillin-Streptomycin (Invitrogen, 15070063). Cells were seeded at a density of approximately 50 000 cells/cm^2 in T25 flasks and passaged upon reaching 80%-90% confluency (typically every 2-3 days).

For genomic DNA isolation, cells were detached, collected, and pelleted by centrifugation at 300 × *g* for 5 min. Genomic DNA was subsequently extracted using the FastPure Blood/Cell/Tissue/Bacteria DNA Isolation Mini Kit (Vazyme, DC112-01) according to the manufacturer's protocol.

4.3. Genomic DNA fragmentation, end repair and adapter ligation

Genomic DNA was fragmented to an average size of around 300 bp using a Covaris M220 Focused-ultrasonicator. Double size selection was performed as needed, following the manufacturer's protocol to enrich fragments in the 300–500 bp range. End repair and A-tailing were performed using the VANTS Universal DNA Library Prep Kit for Illumina V3 (Vazyme, cat. no. ND607) according to the manufacturer's protocol. For PCR-free libraries, full-length Illumina adapters (Vazyme, cat. no. N34201) were ligated to repaired DNA. For methylation libraries, EM-seq adapters (NEB, cat. no. E7140) were used instead.

4.4. General FINE protocol

A 10-μl isothermal amplification reaction was assembled containing the adaptor-ligated DNA, 250 nM each of forward and reverse primers (sequences listed in Table S7), 5% PEG8000 (Beyotime), 2 mM DTT (BioFroxx), 0.4 mM dNTPs (Vazyme), 300 ng/μL T4 gp32 protein (ABclonal), 0.1 U/μL Bsu DNA polymerase (ABclonal), and 0.4 U/μL Nt.BsmAI (NEB), in 1× rCutSmart buffer (NEB). The reaction mix was incubated at 34 °C for 20 min. The amplified products were purified twice using 0.8 × VANTS DNA Clean Beads (Vazyme) and eluted in a low-EDTA buffer (ABclonal). DNA concentration was quantified using the Qubit dsDNA HS Assay Kit (Vazyme).

4.5. Methylation library amplification by FINE or PCR

After adapter ligation, unmethylated cytosines in the DNA were enzymatically converted to uracil using the EpiArt DNA Enzymatic Methylation Kit (Vazyme, cat. no. EM301), following the manufacturer's protocol. The converted DNA was eluted in 9–20 μL of nuclease-free water, adjusted based on downstream application requirements.

For FINE-EM-seq libraries, converted DNA (1 ng, 100 pg, or 10 pg) was amplified under the same isothermal amplification conditions described above, using tr-1 and tr-2 primers (Table S7). To add full-length adapters for Illumina sequencing, the entire FINE reaction product, without any intermediate purification, was indexed using a 3-cycle PCR with 2 × Synthesis Mix (ABclonal) and 0.45 μM each of i5 and i7 indexing primers. The amplified products were purified twice with 0.8 × VANTS DNA Clean Beads.

For PCR methylation libraries, converted DNA was amplified using 2 × Synthesis Mix (ABclonal), HiFi V3 (Vazyme) or KAPA HiFi HotStart Uracil + ReadyMix (Roche). For 2 × Synthesis Mix, PCR thermal cycling consisted of an initial denaturation at 98 °C for 45 s; followed by 16 cycles (for 1 ng), 20 cycles (for 100 pg), or 23 cycles (for 10 pg) of 98 °C for 15 s, 60 °C for 30 s, and 72 °C for 30 s; followed by a final extension at 72 °C for 1 min and then hold at 12 °C. For HiFi V3, PCR thermal cycling consisted of an initial denaturation at 95 °C for 3 min; followed by 14 cycles (for 1 ng), 17 cycles (for 100 pg), or 21 cycles (for 10 pg) of 98 °C for 20 s, 60 °C for 15 s, and 72 °C for 30 s; followed by a final extension at 72 °C for 5 min and then hold at 12 °C. KAPA U amplification was performed with initial denaturation at 95 °C for 3 min, followed by 14 cycles (for 1 ng), 17 cycles (for 100 pg), or 21 cycles (for 10 pg) of 98 °C for 20 s, 60 °C for 15 s, and 72 °C for 30 s, and a final extension at 72 °C for 5 min. The PCR-amplified DNA was purified twice using 0.8 × VANTS DNA Clean Beads.

Additionally, for unconverted genomic DNA libraries, amplification was performed either with the FINE protocol as described above, or with HiFi N616 polymerase (Vazyme) using 8 cycles under the same thermal cycling conditions as HiFi V3.

4.6. Zebrafish genomic DNA isolation and library preparation

Zebrafish were raised and maintained under standard conditions. All experiments were performed according to institutional and national animal welfare guidelines. Embryos were collected at four

developmental stages, namely 64 cell, 128 cell, 1k cell, and Germ ring (gr). Prior to DNA extraction, embryos were bleached with bleach solution (0.1 mL 5% NaClO in 170 mL system water) for 5 min and rinsed thoroughly with 1 × PBS. Genomic DNA was isolated using the FastPure Blood/Cell/Tissue/Bacteria DNA Isolation Mini Kit (Vazyme), according to the manufacturer's protocol. Two biological replicates were collected for each stage.

Genomic DNA from the embryos was fragmented to an average size of around 300 bp using the Bioruptor Pico sonication device (Diagenode). For the 128-cell, 1k-cell, and Germ-ring samples, an optimized sonication program was used, i.e., 15 s ON/30 s OFF, 4 cycles for the 50-μL sample volume. For the 64-cell-stage gDNA, 3 cycles of 15 s ON/30 s OFF were used instead. All fragmented DNA was then purified using 0.8 × VANTS DNA Clean Beads to remove short fragments. Library preparation, enzymatic methylation conversion, and FINE amplification for the zebrafish genomic DNA (using 1 ng converted DNA) were performed in the same way as for the HeLa genomic DNA. All libraries were sequenced as 150-bp paired-end reads on the NovaSeq platform (Illumina).

4.7. Sequencing data pre-processing

Sequencing depth was defined as the total number of bases (read length × number of reads) divided by haploid genome size (Sims et al., 2014). To assess sequencing data quality, per-nucleotide phred scores were calculated and visualized from a random subset of 200,000 reads for each sample using asTair phred (Liu et al., 2019). Adapter and quality filtering were performed with Trim Galore v0.6.10 (https://www.bioinformatics.babraham.ac.uk/projects) (Bolger et al., 2014). Parameters were applied specifically for each sample group: unconverted and converted HeLa were trimmed with default parameters, while WGBS and zebrafish samples were trimmed with -paired –length 35 –clip_R1 10 –clip_R2 15 –three_prime_clip_R 10 –three_prime_clip_R2 10. Trimmed reads were aligned to the human reference genome (GRCh38) or the zebrafish reference genome (GRCz11.114) with spike-in sequences included. Unconverted HeLa genomic DNA libraries were aligned with BWA-MEM v0.7.17 (Li & Durbin, 2009) using default parameters. Converted DNA libraries were aligned using Bismark v0.24.2 (Krueger & Andrews, 2011) with default parameters. Zebrafish samples were aligned using Bismark with –maxins 1000. PCR duplicates were removed using deduplicate_bismark.

Genome coverage statistics were obtained using Picard v3.1.1 (https://broadinstitute.github.io/picard/) function CollectWgsMetrics. We computed GC bias metrics with CollectGCBiasMetrics and insert size distribution with CollectInsertSizeMetrics. Methylation information was extracted from deduplicated BAM files using bismark_methylation_extractor with default settings.

To benchmark FINE with PCR, raw reads were downsampled to an equal number per group using seqtk v1.4 (https://github.com/lh3/seqtk). Per-base coverage tracks (1-bp bins) were generated with bedtools v2.31.1 (Quinlan & Hall, 2010) and converted into BigWig format using deeptools v3.5.4 (Ramírez et al., 2016). In the CpG context, global methylation level was calculated as the number of cytosines that remained unconverted C divided by the total number of cytosines at CpG sites in uniquely mapped reads. Pairwise correlations of CpG methylation levels between libraries were computed using the getCorrelation function in the methylKit R package v1.24.0 (Akalin et al., 2012), reporting Pearson correlation coefficients as density plots.

4.8. Differentially methylated region and AT-rich region analysis

Differentially methylated regions (DMRs) were identified using the methylKit R package with a minimum coverage of 3 × per CpG site, a window size of 1 kb, and a step size of 500 bp. DMRs were categorised as hyper ($meth.diff \geq 10$, $q \leq 0.05$), hypo ($meth.diff \leq -10$, $q \leq 0.05$), or non-significant ($|meth.diff| < 10$ or $q > 0.05$). Here, q-values refer to p-values adjusted using the Sliding Linear Model (SLIM) method implemented in methylKit. DMRs were annotated to nearby genes using the ChIPseeker R package v1.44.0 (Heinz et al., 2010; Yu et al., 2015), and those annotated as intergenic were removed from downstream analysis. Gene Ontology (GO) enrichment was performed with FishEnrichr (Chen et al., 2013; Kuleshov et al., 2016) against the “Coexpression Predicted GO Biological Process 2018” gene set. P-values were calculated using Fisher's exact test (or the hypergeometric test) and adjusted by the Benjamini-Hochberg (BH) method for multiple testing correction. GO terms with BH-adjusted $p < 0.05$ were considered significant.

CpG island annotations for GRCz11 were downloaded from the UCSC Genome Browser (Perez et al., 2025). AT-rich regions were defined as 100-bp genomic windows with GC content < 25%, which were identified by scanning the genome with a 100-bp step size. Overlaps between AT-rich regions and DMRs were assessed with bedtools.

4.9. Statistics

Pairwise correlations of CpG methylation levels between libraries were evaluated using Pearson correlation coefficients. Differentially methylated regions (DMRs) were identified using the methylKit package with a minimum CpG coverage of 3 × . Statistical significance for DMRs was assessed using q-values adjusted by the Sliding Linear Model (SLIM) method, with $q \leq 0.05$ considered significant.

Gene Ontology enrichment analysis was performed using Fisher's exact test (or the hypergeometric test), followed by Benjamini–Hochberg correction for multiple testing. Adjusted p-values < 0.05 were considered statistically significant.

CRediT authorship contribution statement

Chenyang Ding: Writing – review & editing, Writing – original draft, Methodology, Investigation, Formal analysis, Conceptualization, Resources, Data curation, Visualization. **Qifeng Zhang:** Investigation, Formal analysis, Data curation, Writing – review & editing, Writing – original draft, Visualization. **Jing Wang:** Investigation, Resources. **Yanbo Xu:** Investigation, Formal analysis, Writing – original draft, Writing – review & editing, Visualization. **Tiantian Huang:** Investigation, Visualization, Writing – review & editing. **Yanfang Du:** Investigation. **Junjie Zhang:** Investigation, Writing – review & editing, Funding acquisition. **Xiang Zhou:** Supervision. **Yibin Liu:** Supervision, Conceptualization, Resources, Visualization, Project administration, Funding acquisition, Investigation, Writing – review & editing. **Zhiyuan Hu:** Supervision, Conceptualization, Formal analysis, Investigation, Data curation, Resources, Writing – review & editing, Visualization, Project administration, Funding acquisition.

Declaration of competing interest

Y.L., Z.H. and C.D. are inventors on a Chinese patent application related to the method in this study (application number: 202511025533.X). The other authors declare no competing interests.

Acknowledgements

This work was supported by National Natural Science Foundation of China (32500725 to Z.H., 22307099 to Y.L.) and Fundamental Research Funds for the Central Universities (2042025kf0022, 2042022dx0003) to Z.H.. This work was also supported by the Large-scale Instrument and Equipment Sharing Foundation of Wuhan University. The authors thank Dr Ruxiao Xing and the Core Facility of Taikang Center for Life and Medical Sciences, Wuhan University for access to experimental equipment. We thank Yanjun Chen and the HPC Core Facility of Medical Research Institute, Wuhan University for technical support. We also thank Prof Ruilin Zhang and his research group for providing the zebrafish facility and technical support.

Appendix A. Supplementary data

Supplementary data to this article can be found online at https://doi.org/10.1016/j.cellin.2026.100324.

Data availability

The raw and processed data have been deposited to the GEO (accession: GSE307505). The code and analysis scripts are available at https://github.com/zhiyuan-hu-lab/FINE-EM-seq.

References

Aird, D., Ross, M. G., Chen, W. S., Danielsson, M., Fennell, T., Russ, C., Jaffe, D. B., Nusbaum, C., & Gnirke, A. (2011). Analyzing and minimizing PCR amplification bias in Illumina sequencing libraries. *Genome Biology, 12*, R18. https://doi.org/10.1186/gb-2011-12-2-r18

Akalin, A., Kormaksson, M., Li, S., Garrett-Bakelman, F. E., Figueroa, M. E., Melnick, A., & Mason, C. E. (2012). methylKit: A comprehensive R package for the analysis of genome-wide DNA methylation profiles. *Genome Biology, 13*, R87. https://doi.org/10.1186/gb-2012-13-10-r87

Andersen, I. S., Reiner, A. H., Aanes, H., Alestrom, P., & Collas, P. (2012). Developmental features of DNA methylation during activation of the embryonic zebrafish genome. *Genome Biology, 13*, R65. https://doi.org/10.1186/gb-2012-13-7-r65

Asadi, R., & Mollasalehi, H. (2021). The mechanism and improvements to the isothermal amplification of nucleic acids, at a glance. *Analytical Biochemistry, 631*, Article 114260. https://doi.org/10.1016/j.ab.2021.114260

Bagnoli, J. W., Ziegenhain, C., Janjic, A., Wange, L. E., Vieth, B., Parekh, S., Geuder, J., Hellmann, I., & Enard, W. (2018). Sensitive and powerful single-cell RNA sequencing using mcSCRB-seq. *Nature Communications, 9*, 2937. https://doi.org/10.1038/s41467-018-05347-6

Bauer, H., Lele, Z., Rauch, G.-J., Geisler, R., & Hammerschmidt, M. (2001). The type I serine/threonine kinase receptor Alk8/Lost-a-fin is required for Bmp2b/7 signal transduction during dorsoventral patterning of the zebrafish embryo. *Development, 128*, 849–858. https://doi.org/10.1242/dev.128.6.849

Benjamini, Y., & Speed, T. P. (2012). Summarizing and correcting the GC content bias in high-throughput sequencing. *Nucleic Acids Research, 40*, e72. https://doi.org/10.1093/nar/gks001

Bolger, A. M., Lohse, M., & Usadel, B. (2014). Trimmomatic: A flexible trimmer for Illumina sequence data. *Bioinformatics, 30*, 2114–2120. https://doi.org/10.1093/bioinformatics/btu170

Bruce, A. E., & Heisenberg, C.-P. (2020). Mechanisms of zebrafish epiboly: A current view. *Current Topics in Developmental Biology, 136*, 319–341. https://doi.org/10.1016/bs.ctdb.2019.07.001

Chapin, N., Fernandez, J., Poole, J., & Delatte, B. (2022). Anchor-based bisulfite sequencing determines genome-wide DNA methylation. *Communications Biology, 5*, 596. https://doi.org/10.1038/s42003-022-03543-1

Chen, E. Y., Tan, C. M., Kou, Y., Duan, Q., Wang, Z., Meirelles, G. V., Clark, N. R., & Ma'ayan, A. (2013). Enrichr: Interactive and collaborative HTML5 gene list enrichment analysis tool. *BMC Bioinformatics, 14*, 128. https://doi.org/10.1186/1471-2105-14-128

Cui, X. L., Nie, J., Zhu, H., Kowitwanich, K., Beadell, A. V., West-Szymanski, D. C., Zhang, Z., Dougherty, U., Kwesi, A., Deng, Z., Li, Y., Meng, D., Roggin, K., Barry, T., Owyang, R., Fefferman, B., Zeng, C., Gao, L., Zhao, C. W. T., … He, C. (2024). LABS: Linear amplification-based bisulfite sequencing for ultrasensitive cancer detection from cell-free DNA. *Genome Biology, 25*, 157. https://doi.org/10.1186/s13059-024-03262-2

Daher, R. K., Stewart, G., Boissinot, M., & Bergeron, M. G. (2016). Recombinase polymerase amplification for diagnostic applications. *Clinical Chemistry, 62*, 947–958. https://doi.org/10.1373/clinchem.2015.245829

Dai, Q., Ye, C., Irkliyenko, I., Wang, Y., Sun, H. L., Gao, Y., Liu, Y., Beadell, A., Perea, J., Goel, A., & He, C. (2024). Ultrafast bisulfite sequencing detection of 5-methylcytosine in DNA and RNA. *Nature Biotechnology, 42*, 1559–1570. https://doi.org/10.1038/s41587-023-02034-w

Dean, F. B., Hosono, S., Fang, L., Wu, X., Faruqi, A. F., Bray-Ward, P., Sun, Z., Zong, Q., Du, Y., Du, J., Driscoll, M., Song, W., Kingsmore, S. F., Egholm, M., & Lasken, R. S. (2002). Comprehensive human genome amplification using multiple displacement amplification. *Proceedings of the National Academy of Sciences of the United States of America, 99*, 5261–5266. https://doi.org/10.1073/pnas.082089499

Du, Y., Tang, Y., Lin, B., Xue, X., Wang, Y., & Liu, Y. (2023). Bisulfite-free mapping of DNA cytosine modifications: Challenges and perspectives. *Science China Chemistry, 66*, 3044–3053. https://doi.org/10.1007/s11426-023-1729-2

Feng, S., Zhong, Z., Wang, M., & Jacobsen, S. E. (2020). Efficient and accurate determination of genome-wide DNA methylation patterns in Arabidopsis thaliana with enzymatic methyl sequencing. *Epigenetics & Chromatin, 13*, 42. https://doi.org/10.1186/s13072-020-00361-9

Gansauge, M. T., Gerber, T., Glocke, I., Korlevic, P., Lippik, L., Nagel, S., Riehl, L. M., Schmidt, A., & Meyer, M. (2017). Single-stranded DNA library preparation from highly degraded DNA using T4 DNA ligase. *Nucleic Acids Research, 45*, Article e79. https://doi.org/10.1093/nar/gkx033

Gansauge, M. T., & Meyer, M. (2013). Single-stranded DNA library preparation for the sequencing of ancient or damaged DNA. *Nature Protocols, 8*, 737–748. https://doi.org/10.1038/nprot.2013.038

Glökler, J., Lim, T. S., Ida, J., & Frohme, M. (2021). Isothermal amplifications–a comprehensive review on current methods. *Critical Reviews in Biochemistry and Molecular Biology, 56*, 543–586. https://doi.org/10.1080/10409238.2021.1937927

Heinz, S., Benner, C., Spann, N., Bertolino, E., Lin, Y. C., Laslo, P., Cheng, J. X., Murre, C., Singh, H., & Glass, C. K. (2010). Simple combinations of lineage-determining transcription factors prime cis-regulatory elements required for macrophage and B cell identities. *Molecular Cell, 38*, 576–589. https://doi.org/10.1016/j.molcel.2010.05.004

Hu, J., Wang, Y., Ding, H., Jiang, C., Geng, Y., Sun, X., Jing, J., Gao, H., Wang, Z., & Dong, C. (2020). Recombinase polymerase amplification with polymer flocculation sedimentation for rapid detection of Staphylococcus aureus in food samples. *International Journal of Food Microbiology, 331*, Article 108691. https://doi.org/10.1016/j.ijfoodmicro.2020.108691

Ji, L., Sasaki, T., Sun, X., Ma, P., Lewis, Z. A., & Schmitz, R. J. (2014). Methylated DNA is over-represented in whole-genome bisulfite sequencing data. *Frontiers in Genetics, 5*, 341. https://doi.org/10.3389/fgene.2014.00341

Jiang, L., Zhang, J., Wang, J.-J., Wang, L., Zhang, L., Li, G., Yang, X., Ma, X., Sun, X., & Cai, J. (2013). Sperm, but not oocyte, DNA methylome is inherited by zebrafish early embryos. *Cell, 153*, 773–784. https://doi.org/10.1016/j.cell.2013.04.041

Jukam, D., Shariati, S. A. M., & Skotheim, J. M. (2017). Zygotic genome activation in vertebrates. *Developmental Cell, 42*, 316–332. https://doi.org/10.1016/j.devcel.2017.07.026

Kane, D. A., McFarland, K. N., & Warga, R. M. (2005). Mutations in half baked/E-cadherin block cell behaviors that are necessary for teleost epiboly. *Development, 132*, 1105–1116. https://doi.org/10.1242/dev.01668

Kebschull, J. M., & Zador, A. M. (2015). Sources of PCR-induced distortions in high-throughput sequencing data sets. *Nucleic Acids Research, 43*, Article e143. https://doi.org/10.1093/nar/gkv717

Kong, Y., Mead, E. A., & Fang, G. (2023). Navigating the pitfalls of mapping DNA and RNA modifications. *Nature Reviews Genetics, 24*, 363–381. https://doi.org/10.1038/s41576-022-00559-5

Krueger, F., & Andrews, S. R. (2011). Bismark: A flexible aligner and methylation caller for bisulfite-seq applications. *Bioinformatics, 27*, 1571–1572. https://doi.org/10.1093/bioinformatics/btr167

Kuleshov, M. V., Jones, M. R., Rouillard, A. D., Fernandez, N. F., Duan, Q., Wang, Z., Koplev, S., Jenkins, S. L., Jagodnik, K. M., & Lachmann, A. (2016). Enrichr: A comprehensive gene set enrichment analysis web server 2016 update. *Nucleic Acids Research, 44*, W90–W97. https://doi.org/10.1093/nar/gkw377

Lee, M. T., Bonneau, A. R., Takacs, C. M., Bazzini, A. A., DiVito, K. R., Fleming, E. S., & Giraldez, A. J. (2013). Nanog, Pou5f1 and SoxB1 activate zygotic gene expression during the maternal-to-zygotic transition. *Nature, 503*, 360–364. https://doi.org/10.1038/nature12632

Lewis, C. A., Jr., Crayle, J., Zhou, S., Swanstrom, R., & Wolfenden, R. (2016). Cytosine deamination and the precipitous decline of spontaneous mutation during Earth's history. *Proceedings of the National Academy of Sciences of the United States of America, 113*, 8194–8199. https://doi.org/10.1073/pnas.1607580113

Li, H., & Durbin, R. (2009). Fast and accurate short read alignment with burrows-wheeler transform. *Bioinformatics, 25*, 1754–1760. https://doi.org/10.1093/bioinformatics/btp324

Lim, J., Park, C., Kim, M., Kim, H., Kim, J., & Lee, D. S. (2024). Advances in single-cell omics and multiomics for high-resolution molecular profiling. *Experimental and Molecular Medicine, 56*, 515–526. https://doi.org/10.1038/s12276-024-01186-2

Lister, R., Pelizzola, M., Dowen, R. H., Hawkins, R. D., Hon, G., Tonti-Filippini, J., Nery, J. R., Lee, L., Ye, Z., & Ngo, Q.-M. (2009). Human DNA methylomes at base resolution show widespread epigenomic differences. *Nature, 462*, 315–322. https://doi.org/10.1038/nature08514

Liu, Y., Siejka-Zielińska, P., Velikova, G., Bi, Y., Yuan, F., Tomkova, M., Bai, C., Chen, L., Schuster-Böckler, B., & Song, C.-X. (2019). Bisulfite-free direct detection of 5-methylcytosine and 5-hydroxymethylcytosine at base resolution. *Nature Biotechnology, 37*, 424–429. https://doi.org/10.1038/s41587-019-0041-2

Mattei, A. L., Bailly, N., & Meissner, A. (2022). DNA methylation: A historical perspective. *Trends in genetics, 38*, 676–707. https://doi.org/10.1016/j.tig.2022.03.010

Mintzer, K. A., Lee, M. A., Runke, G., Trout, J., Whitman, M., & Mullins, M. C. (2001). Lost-a-fin encodes a type I BMP receptor, Alk8, acting maternally and zygotically in dorsoventral pattern formation. *Development, 128*, 859–869. https://doi.org/10.1242/dev.128.6.859

Notomi, T., Mori, Y., Tomita, N., & Kanda, H. (2015). Loop-mediated isothermal amplification (LAMP): Principle, features, and future prospects. *Journal of Microbiology, 53*, 1–5. https://doi.org/10.1007/s12275-015-4656-9

Okuda, Y., Yoda, H., Uchikawa, M., Furutani-Seiki, M., Takeda, H., Kondoh, H., & Kamachi, Y. (2006). Comparative genomic and expression analysis of group B1 sox genes in zebrafish indicates their diversification during vertebrate evolution. *Developmental Dynamics, 235*, 811–825. https://doi.org/10.1002/dvdy.20678

Olova, N., Krueger, F., Andrews, S., Oxley, D., Berrens, R. V., Branco, M. R., & Reik, W. (2018). Comparison of whole-genome bisulfite sequencing library preparation strategies identifies sources of biases affecting DNA methylation data. *Genome Biology, 19*, 33. https://doi.org/10.1186/s13059-018-1408-2

Oyola, S. O., Otto, T. D., Gu, Y., Maslen, G., Manske, M., Campino, S., Turner, D. J., Macinnis, B., Kwiatkowski, D. P., Swerdlow, H. P., & Quail, M. A. (2012). Optimizing Illumina next-generation sequencing library preparation for extremely AT-biased genomes. *BMC Genomics, 13*, 1. https://doi.org/10.1186/1471-2164-13-1

Perez, G., Barber, G. P., Benet-Pages, A., Casper, J., Clawson, H., Diekhans, M., Fischer, C., Gonzalez, J. N., Hinrichs, A. S., & Lee, C. M. (2025). The UCSC genome browser database: 2025 update. *Nucleic Acids Research, 53*, D1243–D1249. https://doi.org/10.1093/nar/gkae974

Potapov, V., & Ong, J. L. (2017). Examining sources of error in PCR by single-molecule sequencing. *PLoS One, 12*, Article e0169774. https://doi.org/10.1371/journal.pone.0169774

Potok, M. E., Nix, D. A., Parnell, T. J., & Cairns, B. R. (2013). Reprogramming the maternal zebrafish genome after fertilization to match the paternal methylation pattern. *Cell, 153*, 759–772. https://doi.org/10.1016/j.cell.2013.04.030

Qian, C., Wang, R., Wu, H., Ji, F., & Wu, J. (2019). Nicking enzyme-assisted amplification (NEAA) technology and its applications: A review. *Analytica Chimica Acta, 1050*, 1–15. https://doi.org/10.1016/j.aca.2018.10.054

Quinlan, A. R., & Hall, I. M. (2010). BEDTools: A flexible suite of utilities for comparing genomic features. *Bioinformatics, 26*, 841–842. https://doi.org/10.1093/bioinformatics/btq033

Ramírez, F., Ryan, D. P., Grüning, B., Bhardwaj, V., Kilpert, F., Richter, A. S., Heyne, S., Dündar, F., & Manke, T. (2016). deepTools2: A next generation web server for deep-sequencing data analysis. *Nucleic Acids Research, 44*, W160–W165. https://doi.org/10.1093/nar/gkw257

Reck-Peterson, S. L., Redwine, W. B., Vale, R. D., & Carter, A. P. (2018). The cytoplasmic dynein transport machinery and its many cargoes. *Nature Reviews Molecular Cell Biology, 19*, 382–398. https://doi.org/10.1038/s41580-018-0004-3

Reid, M. S., Paliwoda, R. E., Zhang, H., & Le, X. C. (2018). Reduction of background generated from template-template hybridizations in the exponential amplification reaction. *Analytical Chemistry, 90*, 11033–11039. https://doi.org/10.1021/acs.analchem.8b02788

Sasaki, Y., Miyoshi, D., & Sugimoto, N. (2006). Effect of molecular crowding on DNA polymerase activity. *Biotechnology Journal, 1*, 440–446. https://doi.org/10.1002/biot.200500032

Schmidt, R., Strähle, U., & Scholpp, S. (2013). Neurogenesis in zebrafish–from embryo to adult. *Neural Development, 8*, 3. https://doi.org/10.1186/1749-8104-8-3

Schulz, K. N., & Harrison, M. M. (2019). Mechanisms regulating zygotic genome activation. *Nature Reviews Genetics, 20*, 221–234. https://doi.org/10.1038/s41576-018-0087-x

Shimizu, T., Yabe, T., Muraoka, O., Yonemura, S., Aramaki, S., Hatta, K., Bae, Y.-K., Nojima, H., & Hibi, M. (2005). E-cadherin is required for gastrulation cell movements in zebrafish. *Mechanisms of Development, 122*, 747–763. https://doi.org/10.1016/j.mod.2005.03.008

Sims, D., Sudbery, I., Ilott, N. E., Heger, A., & Ponting, C. P. (2014). Sequencing depth and coverage: Key considerations in genomic analyses. *Nature Reviews Genetics, 15*, 121–132. https://doi.org/10.1038/nrg3642

Song, Z., Hu, K., Rao, J., Cheng, B., Xu, L., An, R., & Liang, X. (2023). Unexpected mechanism and inhibition effect for nonspecific amplification involving dynamic binding of primers with background DNA. *Analytical Chemistry, 95*, 16819–16829. https://doi.org/10.1021/acs.analchem.3c02274

Srivastava, P., & Prasad, D. (2023). Isothermal nucleic acid amplification and its uses in modern diagnostic technologies. *3 Biotech, 13*, 200. https://doi.org/10.1007/s13205-023-03628-6

Stackley, K. D., Beeson, C. C., Rahn, J. J., & Chan, S. S. (2011). Bioenergetic profiling of zebrafish embryonic development. *PLoS One, 6*, Article e25652. https://doi.org/10.1371/journal.pone.0025652

Tan, M., Liao, C., Liang, L., Yi, X., Zhou, Z., & Wei, G. (2022). Recent advances in recombinase polymerase amplification: Principle, advantages, disadvantages and applications. *Frontiers in Cellular and Infection Microbiology, 12*, Article 1019071. https://doi.org/10.3389/fcimb.2022.1019071

Tan, S. C., Scherer, J., & Vallee, R. B. (2011). Recruitment of dynein to late endosomes and lysosomes through light intermediate chains. *Molecular Biology of the Cell, 22*, 467–477. https://doi.org/10.1091/mbc.E10-02-0129

Urich, M. A., Nery, J. R., Lister, R., Schmitz, R. J., & Ecker, J. R. (2015). MethylC-seq library preparation for base-resolution whole-genome bisulfite sequencing. *Nature Protocols, 10*, 475–483. https://doi.org/10.1038/nprot.2014.114

Vaisvila, R., Ponnaluri, V. C., Sun, Z., Langhorst, B. W., Saleh, L., Guan, S., Dai, N., Campbell, M. A., Sexton, B. S., & Marks, K. (2021). Enzymatic methyl sequencing detects DNA methylation at single-base resolution from picograms of DNA. *Genome Research, 31*, 1280–1289. https://doi.org/10.1101/gr.266551.120

Wang, J., Fang, Y., Chen, W., Zhang, C., Chen, Z., Xie, Z., Weng, Z., Chen, W., Ruan, F., & Xie, Y. (2022). *High coverage of single cell genomes by T7-assisted enzymatic methyl-sequencing*. Preprint at https://www.biorxiv.org/content/10.1101/2022.02.23.481567v1.

Wang, X., Yu, B., Sakurabayashi, S., Paz-Villatoro, J. M., & Iwahara, J. (2024). Robust enzymatic production of DNA G-quadruplex, aptamer, DNAzyme, and other oligonucleotides: Applications for NMR. *Journal of the American Chemical Society, 146*, 1748–1752. https://doi.org/10.1021/jacs.3c11219

Wu, X., Zhang, H., Zhang, B., Zhang, Y., Wang, Q., Shen, W., Wu, X., Li, L., Xia, W., & Nakamura, R. (2021). Methylome inheritance and enhancer dememorization reset an epigenetic gate safeguarding embryonic programs. *Science Advances, 7*, Article eabl3858. https://doi.org/10.1126/sciadv.abl3858

Yamada, K., Maeno, A., Araki, S., Kikuchi, M., Suzuki, M., Ishizaka, M., Satoh, K., Akama, K., Kawabe, Y., & Suzuki, K. (2021). An atlas of seven zebrafish hox cluster mutants provides insights into sub/neofunctionalization of vertebrate hox clusters. *Development, 148*, dev198325. https://doi.org/10.1242/dev.198325

Yu, G., Wang, L.-G., & He, Q.-Y. (2015). ChIPseeker: An R/Bioconductor package for ChIP peak annotation, comparison and visualization. *Bioinformatics, 31*, 2382–2383. https://doi.org/10.1093/bioinformatics/btv145

Zhang, Y., Luck, A. N., & Tanner, N. A. (2024). Isothermal amplification of long DNA fragments at low temperature by improved strand displacement amplification. *Biotechniques, 76*, 255–262. https://doi.org/10.2144/btn-2024-0012

Zhang, Y., & Tanner, N. A. (2017). Isothermal amplification of long, discrete DNA fragments facilitated by single-stranded binding protein. *Scientific Reports, 7*, 8497. https://doi.org/10.1038/s41598-017-09063-x

Zhu, Z., Samuelson, J. C., Zhou, J., Dore, A., & Xu, S. Y. (2004). Engineering strand-specific DNA nicking enzymes from the type IIS restriction endonucleases BsaI, BsmBI, and BsmAI. *Journal of Molecular Biology, 337*, 573–583. https://doi.org/10.1016/j.jmb.2004.02.003

Zyrina, N. V., & Antipova, V. N. (2021). Nonspecific synthesis in the reactions of isothermal nucleic acid amplification. *Biochemistry (Mosc), 86*, 887–897. https://doi.org/10.1134/S0006297921070099

Zyrina, N. V., Artiukh, R. I., Svad'bina, I. V., Zheleznaia, L. A., & Matvienko, N. I. (2012). [Effect of single-stranded DNA binding proteins on template/primer-independent DNA synthesis in the presence of nicking endonuclease Nt.BspD6I]. *Bioorganicheskaia Khimiia, 38*, 199–205. https://doi.org/10.1134/s1068162012020161